

Mixed Convection Flow across a Vertical Cone with Heat Source/Sink and Chemical Reaction Effects

Om Prakash Meena^{a,*}, Pranitha Janapatla^b, and D. Srinivasacharya^b

^a*Department of Mathematics, Shaheed Bhagat Singh College, University of Delhi, New Delhi, 110017 India*

^b*Department of Mathematics, National Institute of Technology Warangal, Telangana, 506004 India*

*e-mail: omi.omprakash95@gmail.com

Received June 21, 2021; revised June 21, 2021; accepted August 30, 2021

Abstract—This contribution is concerned with mixed convection flow across a vertical cone in the presence of heat source/sink and chemical reaction effects; the two-dimensional, steady, laminar, viscous incompressible fluid flow case has been discussed with favorable applications in the science, engineering, and industries. The flow model is designed in the form of mathematical equations and, for the sake of numerical solution simplicity, non-dimensionalization has been performed and the gained non-similarity equations are solved numerically via an efficient numerical technique called the bivariate Chebyshev spectral collocation quasi-linearization method. A schematic illustration of the obtained results at various stream-wise locations of the velocity, temperature, and concentration profiles for variations of the governing parameters are exhibited in the results and discussions section; and we have noted that higher rate of heat generation made heat transfer to the surface from the flow, and it enhances temperature profile as well. Moreover, skin friction, heat, and mass transfer rate are also illustrated in tabular form. To authenticate the accuracy of the present computations, we organize a favorable comparison with prior published computation; the residual analysis study also depicted which determines the convergence of the framed numerical simulation.

Keywords: mixed convection, vertical cone, heat source/sink effect, chemical reaction effect, bivariate Chebyshev spectral collocation quasi-linearization method

DOI: 10.1134/S2070048222030127

1. INTRODUCTION

The boundary layer theory on mixed convection flow became most trendy portion nowadays and the heat source/sink is a key in this portion which has countless application in science, engineering, and industries; like, it's presence may shift the temperature distribution in the fluid which alters the particle deposition rate in systems such as electronic chips, nuclear reactors, semiconductors, heat exchangers, nuclear waste disposal, and many more. This core of specialization has brought several researchers and many of them have worked on various shapes and flow models, some of them can be like: Yih [1] analyses heat source/sink effect over vertical permeable plate for MHD mixed convection stagnation flow. Heat transfer with viscous dissipation over a stretching sheet in a micropolar fluid was examined by Mohamadein and Gorla [2]. Ibrahim et al. [3] introduced unsteady MHD natural convection flow over a semi-infinite vertical permeable moving plate with radiation absorption and chemical reaction presence. An analysis of hydromagnetic flow over a stretching vertical surface with chemical reaction and hall current was proposed by Salem and El-Aziz [4]. Das et al. [5] presented a heat transfer analysis across a vertical porous plate of MHD flow in the presence of mass transfer effect. A mixed convection flow across a moving vertical plate with double diffusive and chemical reaction was presented by Patil et al. [6]. An analysis of heat transfer across vertical plate in a parallel free stream flow also introduced by Patil et al. [7]. Ibrahim and Shanker [8] considered boundary-layer flow over stretching sheet of an unsteady MHD flow. An analysis of heat and mass transfer of a visco-elastic fluid through porous medium was introduced by Mishra et al. [9]. Jena et al. [10] proposed MHD viscoelastic fluid flow over a vertical stretching sheet with chemical reaction effect. A natural convection flow over an infinite isothermal vertical plate in the presence of chemical reaction and thermal diffusion effects were examined by Islam and Ahmed [11].

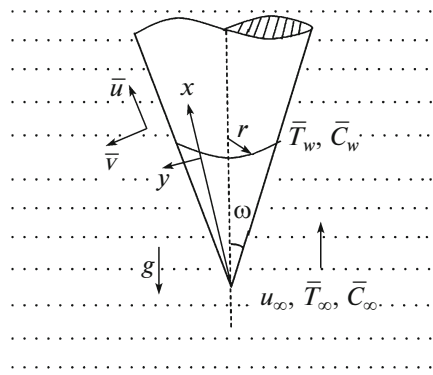


Fig. 1. Coordinate system and physical model.

Another segment in this manuscript is the chemical reaction impact which is also an essential terminology with vast applications in many transport processes; it appears in the water and air pollution, in nuclear reactor safety and combustion systems, fibrous insulation, solar collectors, atmospheric flows, chemical, and metallurgical engineering problems. If the reaction is directly proportional to the concentration, then called the first-order chemical reaction that we have considered here. A bit of research work has focused on it by numerous researchers on various geometries, few of them can be seen as; Nayak et al. [12] introduced an axisymmetric flow across a radially stretched sheet. A nonlinear boundary layer flow over a porous shrinking sheet in the presence of suction flow was proposed by Muhaimina et al. [13]. Nayak [14] analyzed MHD viscoelastic fluid across a stretching sheet saturated porous medium. An unsteady MHD flow with viscous dissipation effect over a semi-infinite vertical porous plate was proposed by Rao and Shivaiah [15]. Mahapatra et al. [16] studied natural convection flow in a bounded porous medium by a vertical surface. A natural convection MHD flow with slip flow region in a bounded porous medium over a vertical surface was examined by Senapati et al. [17]. Bhattacharyya and Layek [18] presented an MHD boundary layer flow with suction/blowing over a flat plate. A list of study can have seen here Subhas et al. [19, 20], Pal and Chatterjee [21], Nandeppanavar et al. [22], Noor et al. [23], Sharma [24], Srinivasacharya et al. [25], Mabood et al. [26], Hayat et al. [27] and Meena et al. [28–36] which ignored the chemical reaction impact, and it makes a situation to consider it throughout this manuscript.

It has been recognized throughout the existing literature that the study of mixed convection flow across a vertical cone with heat source/sink and chemical reaction effects together have not been examined by any researcher so far, which cannot be negated due to essential key application and the authors have targeted it throughout this contribution.

We compose this work as follows. In Section 2, we propose the geometry and mathematical formulation of the problem. In Section 3, we illustrate the numerical approach, while results and discussions are disclosed in Section 4, and we concluded in Section 5.

2. MATHEMATICAL FORMULATION

Consider a vertical cone with a half-angle ω saturated porous medium on a laminar steady two-dimensional mixed convection flow of a viscous incompressible fluid. The surface of the cone with its generator is aligned with x -axis and y -axis is normal to the surface. The flow moves in an upward direction, parallel to the axis of the cone. T_∞ and C_∞ are uniform temperature and concentration in the ambient region, and T_w and C_w are at the surface of the cone, respectively. Where $T_w < T_\infty$ corresponds to a cooled cone, $T_w > T_\infty$ correspond to a heated cone. u_∞ is the uniform stream velocity in the ambient region. We consider heat source/sink and first-order chemical reaction impacts for better analysis of the heat and mass transfer. An illustration of the flow model and coordinates system is pictured in Fig. 1. We assumed that all the fluid properties are constant except the density variation in temperature and concentration (Boussinesq's approximation).

The governing equations of the model are as follows, see [37, 38]:

$$\frac{\partial \bar{u}}{\partial x} + \frac{\partial \bar{v}}{\partial y} = 0, \quad (1)$$

$$\bar{u} \frac{\partial \bar{u}}{\partial x} + \bar{v} \frac{\partial \bar{u}}{\partial y} = U \frac{dU}{dx} + \nu \frac{\partial^2 \bar{u}}{\partial y^2} + gK \cos \omega (\beta_T (\bar{T} - \bar{T}_\infty) - \beta_C (\bar{C} - \bar{C}_\infty)), \quad (2)$$

$$\bar{u} \frac{\partial \bar{T}}{\partial x} + \bar{v} \frac{\partial \bar{T}}{\partial y} = \frac{k}{\rho C_p} \frac{\partial^2 \bar{T}}{\partial y^2} + \frac{Q_0}{\rho C_p} (\bar{T} - \bar{T}_\infty), \quad (3)$$

$$\bar{u} \frac{\partial \bar{C}}{\partial x} + \bar{v} \frac{\partial \bar{C}}{\partial y} = D_e \frac{\partial^2 \bar{C}}{\partial y^2} - K_c (\bar{C} - \bar{C}_\infty). \quad (4)$$

Boundary conditions are:

$$\begin{aligned} \bar{u} = 0, \quad \bar{v} = 0, \quad \bar{T}(x, y) = \bar{T}_w, \quad \bar{C}(x, y) = \bar{C}_w \quad \text{at} \quad y = 0, \\ \bar{u} \rightarrow U = u_\infty x^m, \quad \bar{T}(x, y) \rightarrow \bar{T}_\infty, \quad \bar{C}(x, y) \rightarrow \bar{C}_\infty, \quad \text{as} \quad y \rightarrow \infty, \end{aligned} \quad (5)$$

where, \bar{u} and \bar{v} are velocity components in x and y directions. ω is the half-angle of the cone, \bar{T} is the fluid temperature, \bar{C} is the concentration, ν is the kinematic viscosity, g is the gravitational acceleration, K is the permeability coefficient of the porous medium; β_T and β_C are volumetric coefficients of the thermal and concentration expansions, respectively. D_e is the effective solute diffusivity; k is the thermal conductivity of the fluid, C_p is the specific heat at the constant temperature, Q_0 is the volumetric heat generation or absorption rate, and K_c is the chemical reaction rate.

Introducing the following non-dimensional variables:

$$\begin{aligned} \xi(x) = \left(\frac{2}{m+1} \frac{\nu x}{U} \right)^{1/2}, \quad \eta(x, y) = y \left(\frac{m+1}{2} \frac{U}{\nu x} \right)^{1/2}, \\ \psi(x, y) = \left(\frac{2}{m+1} \nu x U \right)^{1/2} f(\xi, \eta), \\ \bar{T}(x, y) = (\bar{T}_w - \bar{T}_\infty) \theta(\xi, \eta) + \bar{T}_\infty, \quad \bar{C}(x, y) = (\bar{C}_w - \bar{C}_\infty) \phi(\xi, \eta) + \bar{C}_\infty. \end{aligned} \quad (6)$$

By the definition of stream function, we introduce as:

$$\bar{u} = \frac{\partial \psi}{\partial y} \quad \text{and} \quad \bar{v} = -\frac{\partial \psi}{\partial x}. \quad (7)$$

Thus, we have:

$$\bar{u} = U \frac{\partial f}{\partial \eta}, \quad \bar{v} = -\frac{1}{2} \left(\frac{2}{m+1} \frac{\nu U}{x} \right)^{1/2} \left[(m+1)f + (m-1) \left(\eta \frac{\partial f}{\partial \eta} - \xi \frac{\partial f}{\partial \xi} \right) \right]. \quad (8)$$

Enforcing Eqs. (6)–(8) into Eqs. (2)–(4), we get the following forms, respectively,

$$\begin{aligned} \frac{\partial^3 f}{\partial \eta^3} + \frac{2m}{m+1} \left(1 - \left(\frac{\partial f}{\partial \eta} \right)^2 \right) + f \frac{\partial^2 f}{\partial \eta^2} + \frac{2}{m+1} \frac{\lambda}{\text{Pr}} (\theta + N\phi) \\ = \xi \left(\frac{m-1}{m+1} \right) \left(\frac{\partial^2 f}{\partial \eta^2} \frac{\partial f}{\partial \xi} - \frac{\partial f}{\partial \eta} \frac{\partial}{\partial \xi} \left(\frac{\partial f}{\partial \eta} \right) \right), \end{aligned} \quad (9)$$

$$\frac{\partial^2 \theta}{\partial \eta^2} + \text{Pr} f \frac{\partial \theta}{\partial \eta} + \xi^2 Q\theta = \text{Pr} \left(\frac{m-1}{m+1} \right) \xi \left(\frac{\partial \theta}{\partial \eta} \frac{\partial f}{\partial \xi} - \frac{\partial f}{\partial \eta} \frac{\partial \theta}{\partial \xi} \right), \quad (10)$$

$$\frac{\partial^2 \phi}{\partial \eta^2} + \text{Sc} f \frac{\partial \phi}{\partial \eta} - \text{Sc} \xi^2 \Delta \phi = \text{Sc} \left(\frac{m-1}{m+1} \right) \xi \left(\frac{\partial \phi}{\partial \eta} \frac{\partial f}{\partial \xi} - \frac{\partial f}{\partial \eta} \frac{\partial \phi}{\partial \xi} \right). \quad (11)$$

The boundary conditions Eq. (5) are reduced as:

$$\begin{aligned} \frac{\partial f(\xi, \eta)}{\partial \eta} = 0, \quad f(\xi, \eta) - \left(\frac{m-1}{m+1}\right)\xi \frac{\partial f(\xi, \eta)}{\partial \xi} = 0, \quad \theta(\xi, \eta) = 1, \quad \phi(\xi, \eta) = 1 \quad \text{at} \quad \eta = 0, \\ \frac{\partial f(\xi, \eta)}{\partial \eta} \rightarrow 1, \quad \theta(\xi, \eta) \rightarrow 0, \quad \phi(\xi, \eta) \rightarrow 0 \quad \text{as} \quad \eta \rightarrow \infty; \end{aligned} \tag{12}$$

here, $\lambda = \frac{Gr}{Re_x^2}$ is the buoyancy parameter, $N = \frac{\beta_{\bar{C}}(\bar{C}_w - \bar{C}_\infty)}{\beta_{\bar{T}}(\bar{T}_w - \bar{T}_\infty)}$ is the buoyancy ratio, $Ra_x = \frac{gK\beta_T x^2 (\bar{T}_w - \bar{T}_\infty) \cos \omega}{\nu \alpha}$ is the modified local Rayleigh number, $Gr = \frac{Ra_x}{Pr}$ is the local Grashof number, $Re_x = \frac{Ux}{\nu}$ is the local Reynold number, $Pr = \frac{\nu}{\alpha_m}$ is the Prandtl number, $Q = \frac{Q_0}{k}$ is the heat source parameter, $Sc = \frac{\nu}{D_e}$ is the Schmidt number, $\Delta = \frac{K_c}{\nu}$ is the chemical reaction parameter.

The principal bodily quantities of interest which can no longer be skipped are skin friction, heat and mass transfer rates in terms of local skin friction coefficient C_f , local Nusselt number Nu_x , and local Sherwood number Sh_x can be written as:

$$C_f = \frac{2\tau_w}{\rho U^2}, \quad Nu_x = \frac{q_w}{(\bar{T}_w - \bar{T}_\infty)k} x, \quad \text{and} \quad Sh_x = \frac{q_m}{(\bar{C}_w - \bar{C}_\infty)D_f} x;$$

here, $\tau_w = \mu \left(\frac{\partial \bar{u}}{\partial y}\right)_{y=0}$, $q_w = -k_e \left(\frac{\partial \bar{T}}{\partial y}\right)_{y=0}$, and $q_m = -D_e \left(\frac{\partial \bar{C}}{\partial y}\right)_{y=0}$ are defined as wall skin friction, heat flux and mass flux, respectively.

Thus, we have

$$C_f Re_x^{1/2} = 2 \left(\frac{m+1}{2}\right)^{1/2} f''(\xi, 0), \tag{13}$$

$$Nu_x Re_x^{-1/2} = -\left(\frac{m+1}{2}\right)^{1/2} \theta'(\xi, 0), \tag{14}$$

$$Sh_x Re_x^{-1/2} = -\left(\frac{m+1}{2}\right)^{1/2} \phi'(\xi, 0). \tag{15}$$

3. NUMERICAL SOLUTION

The non-similar equations are solved numerically through the well explained numerical technique call the bivariate Chebyshev spectral collocation quasi-linearization method by Meena et al. [39, 40], Magagula et al. [41]. To test the efficiency of the numerical technique; the residual analysis study is computed, which converges up to 10^{-9} .

4. RESULTS AND DISCUSSIONS

In this section the appropriate computations for the non-similarity solution of Eqs. (9)–(11) with the boundary condition Eq. (12) are presented via well explained numerical technique called as bivariate Chebyshev spectral collocation quasi-linearization method (BSQLM). The outcomes are computed in various ranges of the governing parameters: $0 \leq m \leq 1/2$, $0.733 \leq Pr \leq 6.7$, $1.0 \leq \lambda \leq 7.0$, $0.66 \leq Sc \leq 2.57$, $0 \leq Q \leq 2.0$, $-2.0 \leq \Delta \leq 2.0$, $0 \leq \xi \leq 1.0$ and $-2.0 \leq N \leq 2.0$. The edge of boundary layer region η_∞ is carried in between 4.0 to 5.0 according to suitability of computations. To validate the accuracy of the adopted numerical technique, we examined the residual analysis study also which determined the convergence or error of the results and accomplished a perfect convergence after 7th iteration.

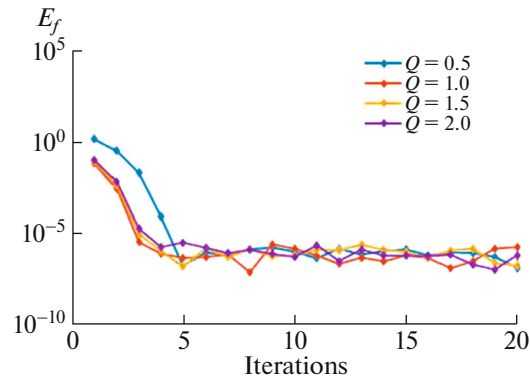


Fig. 2. Residual analysis of $f'(\xi, \eta)$.

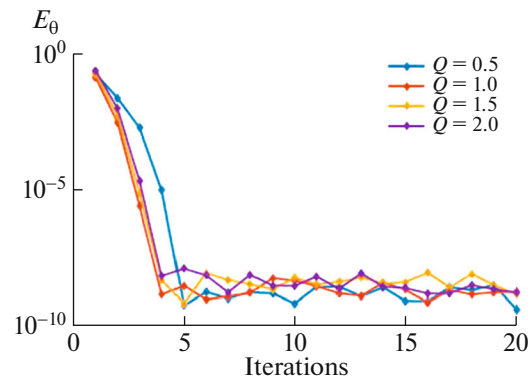


Fig. 3. Residual analysis of $\theta(\xi, \eta)$.

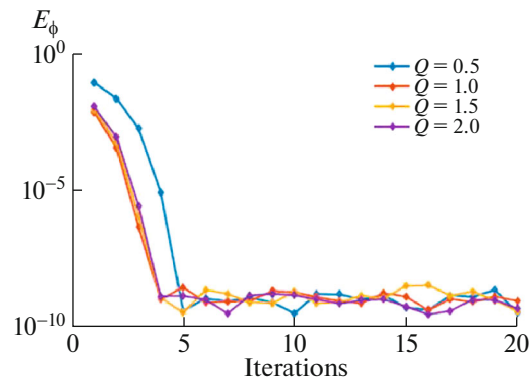


Fig. 4. Residual analysis of $\phi(\xi, \eta)$.

Figures 2–4 present the residual analysis over iterations of $f'(\xi, \eta)$, $\theta(\xi, \eta)$, and $\phi(\xi, \eta)$ for variation of Q with $m = 1/2$, $Pr = 0.733$, $\lambda = 1.0$, $\Delta = 0.5$, $Sc = 0.66$, and $N = 1.0$, respectively. It measures the convergence of the adopted numerical technique. In Fig. 2, we observe that the method converges after nine iterations for variation of Q to 10^{-6} , while in Fig. 3 the method converges after seven iterations for variation of Q to 10^{-9} and in Fig. 4 the method converges after six iterations for variation of Q to 10^{-9} . This justifies the stability and convergence of the method, and, hence, the results are accurate to approximately eight digits.

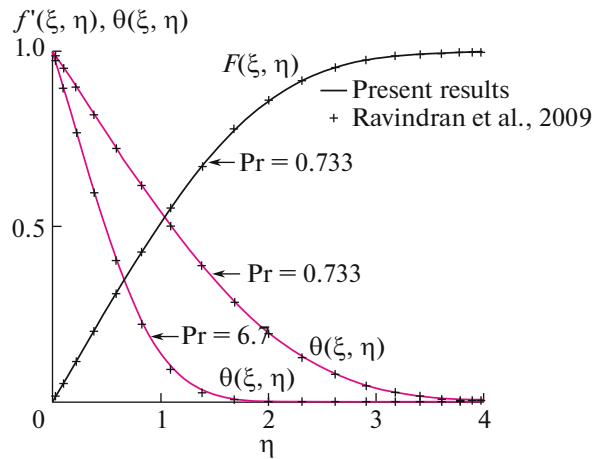


Fig. 5. Comparison of $f'(\xi, \eta)$ and $\theta(\xi, \eta)$ profiles with Ravindran et al. [37].

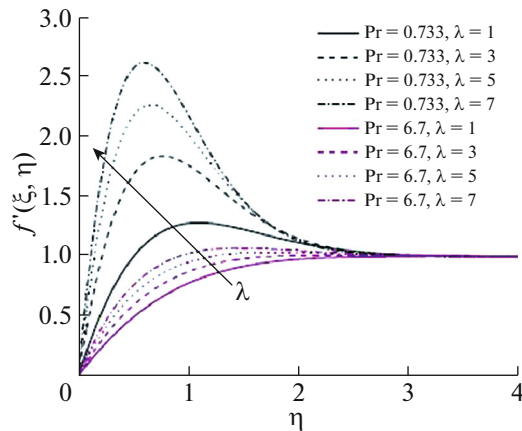


Fig. 6. $f'(\xi, \eta)$ profile for Pr and λ .

Figure 5 presents a comparison of $f'(\xi, \eta)$ and $\theta(\xi, \eta)$ profiles for Pr with prior published results Ravindran et al. [37], through this, we can recognize the agreement of present and past results that verifies working efficiency of the adopted technique code in the MATLAB.

Figures 6–8 proposes $f'(\xi, \eta)$, $\theta(\xi, \eta)$, and $\phi(\xi, \eta)$ for variation of Pr and λ together with $m = 1/2$, $Q = 1.0$, $\Delta = 0.5$, $Sc = 0.66$, and $N = 1.0$. In Fig. 6, $f'(\xi, \eta)$ profile enhances with λ and for low values of Pr = 0.733 a sudden higher growth rate is observed close to cone surface, but it doesn't occur for Pr = 6.7 that is caused by the low viscosity of the fluid. In Figs. 7 and 8, $\theta(\xi, \eta)$ and $\phi(\xi, \eta)$ profiles decrease with an increment in λ , respectively, but $\phi(\xi, \eta)$ profile is contrary with Pr, i.e., increases, while $f'(\xi, \eta)$ and $\theta(\xi, \eta)$ profiles decrease. It can be noted from Figs. 6–8 that all the profiles growth or shrinking rates are greater in magnitude with the small Pr = 0.733 because Pr is the ratio in between kinematic viscosity and thermal diffusivity and increment in this refers to increment in the fluid viscosity, thus the buoyancy λ become more dominant on low viscosity (Pr = 0.733) fluid comparing to higher (Pr = 6.7).

Figures 9–11 examines $f'(\xi, \eta)$, $\theta(\xi, \eta)$, and $\phi(\xi, \eta)$ boundary layer profiles, for variation of Pr and Q together with $m = 1/2$, $\lambda = 1.0$, $\Delta = 0.5$, $Sc = 0.66$, and $N = 1.0$. In Fig. 9, $f'(\xi, \eta)$ profile decreases with Q for heat absorption case $Q < 0$ but contrary for heat generation case $Q > 0$, i.e. enhances; while in Fig. 10, $\theta(\xi, \eta)$ profile also decreases with $Q < 0$ and enhances with $Q > 0$ due to higher heat in the flow region, the flow particles interaction or velocity enhanced and that causes a reduction or acceleration in

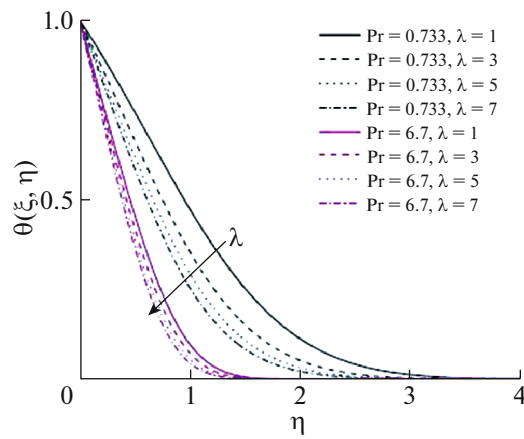


Fig. 7. $\theta(\xi, \eta)$ profile for Pr and λ .

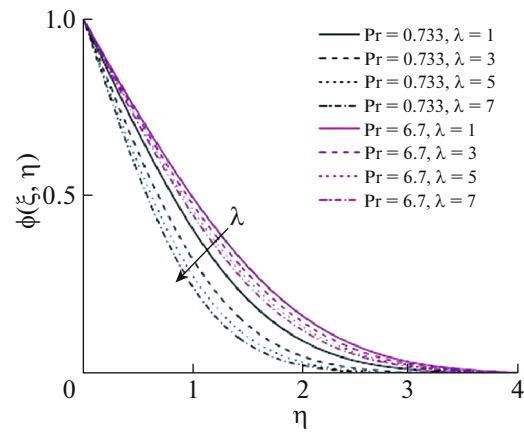


Fig. 8. $\phi(\xi, \eta)$ profile for Pr and λ .

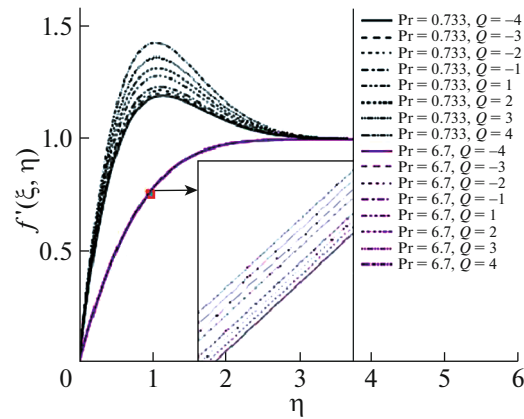


Fig. 9. $f'(\xi, \eta)$ profile for Pr and Q .

Fig. 9 also; in Fig. 11, $\phi(\xi, \eta)$ profile boosts with Q (in $Q < 0$ case) and decreases with Q (in $Q > 0$ case). In Figs. 9–10 we can note a similar tendency on $f'(\xi, \eta)$ and $\theta(\xi, \eta)$ profiles with Pr, i.e., decrease with Pr but $\phi(\xi, \eta)$ profile in Fig. 11 has contrary trend, i.e., increases with Pr; we can notice that the shrinking

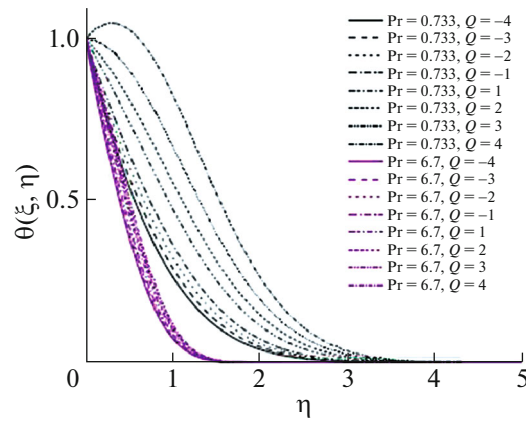


Fig. 10. $\theta(\xi, \eta)$ profile for Pr and Q .

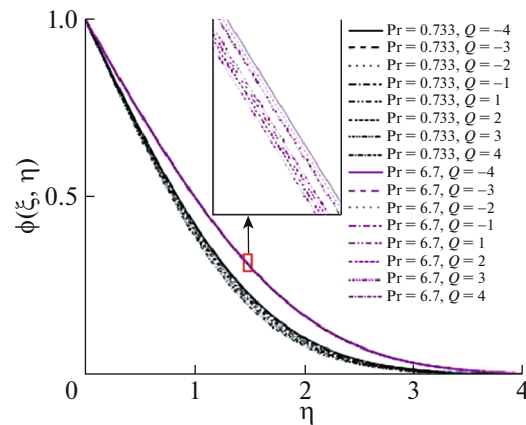


Fig. 11. $\phi(\xi, \eta)$ profile for Pr and Q .

or speeding up rates are higher in magnitude at low Pr (=0.733) compared to the higher one Pr (=6.7) and an increment in Pr reflects fluid viscosity increment; therefore, we can conclude that the heat generation/absorption impact is more prevailing in low viscosity fluid comparing to a higher one.

Figures 12–14 reflects $f'(\xi, \eta)$, $\theta(\xi, \eta)$, and $\phi(\xi, \eta)$ profiles for Pr and m variation together with $Q = 1.0$, $\lambda = 1.0$, $\Delta = 0.5$, $Sc = 0.66$, and $N = 1.0$; $m = \frac{\omega}{\pi - \omega}$; here, ω is the half-angle of the cone (for brief discussion, see Ravindran and Ganapathirao [42]); this implies the values of $m = [0, 0.2, 0.3, 0.5]$ typically represent half-angle of the cone $[0, 30, 45, 60]$ degrees, respectively; therefore, an increment in m refers increment in the half-angle ω of the cone. In Fig. 12, $f'(\xi, \eta)$ profile decreases with m at Pr = 0.733, but, on the contrary, at Pr = 6.7 it increases Pr is the ratio in between kinematic viscosity and thermal diffusivity and an increment in Pr means an increment in the kinematic viscosity and reduction in thermal diffusivity; hence, velocity profile $f'(\xi, \eta)$ decreases with the increment in the cone half-angle in the low viscosity fluid Pr = 0.733, but, on the contrary, in the higher viscosity fluid (Pr = 6.7) it enhances. In Fig. 13, $\theta(\xi, \eta)$ profile enhances with m in low viscosity fluid, but has a reverse behavior in higher viscosity fluid, i.e., decreases, and in Fig. 14, $\phi(\xi, \eta)$ profile enhances with m at Pr = 0.733 and reduces at Pr = 6.7. We can conclude from Figs. 12–14 that impact of m is more dominating in low viscosity fluid compared to the higher and the enhancement and shrinking rates are higher in magnitude at Pr = 0.733.

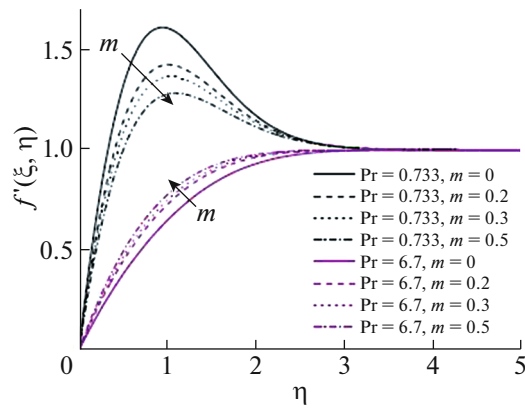


Fig. 12. $f'(\xi, \eta)$ profile for Pr and m .

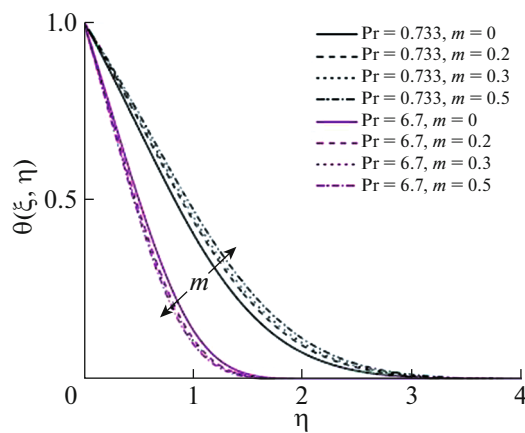


Fig. 13. $\theta(\xi, \eta)$ profile for Pr and m .

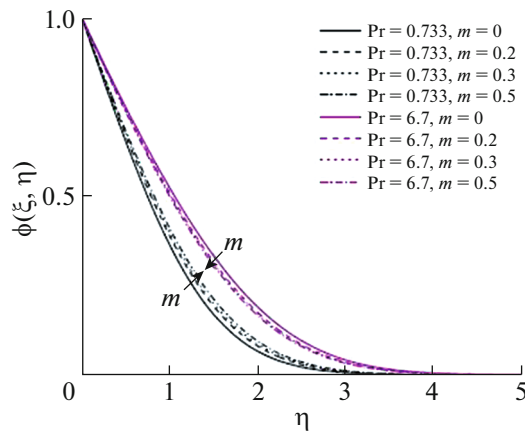


Fig. 14. $\phi(\xi, \eta)$ profile for Pr and m .

Figures 15–17 presents $f'(\xi, \eta)$, $\theta(\xi, \eta)$, and $\phi(\xi, \eta)$ profiles for variation of Sc and Δ together with $Q = 1.0$, $\lambda = 1.0$, $m = 1/2$, $Pr = 0.733$, and $N = 1.0$. In Fig. 17, $\phi(\xi, \eta)$ profile enhances with Δ (in consumption chemical reaction case $\Delta < 0$) that increases $f'(\xi, \eta)$ profile also in Fig. 15, but $\theta(\xi, \eta)$ profile

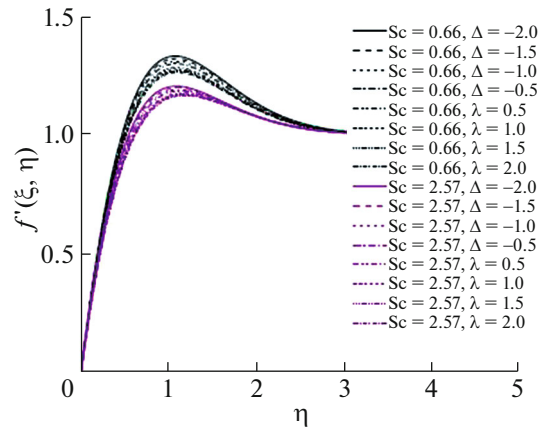


Fig. 15. $f'(\xi, \eta)$ profile for Sc and Δ .

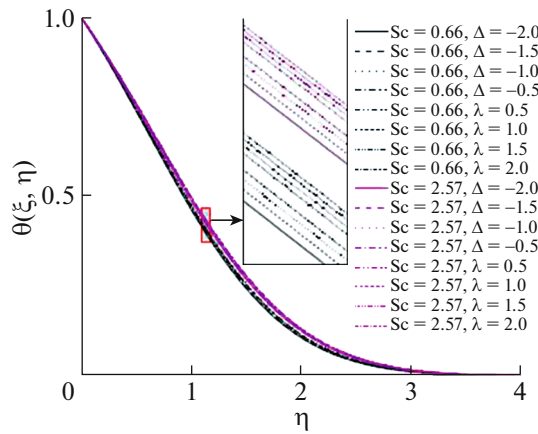


Fig. 16. $\theta(\xi, \eta)$ profile for Sc and Δ .

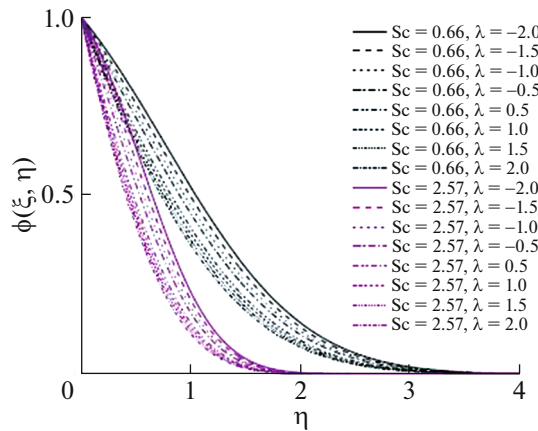


Fig. 17. $\phi(\xi, \eta)$ profile for Sc and Δ .

is contrary, i.e., decreases with Δ (in consumption chemical reaction case $\Delta < 0$) in Fig. 16; but Δ (in generation chemical reaction case $\Delta > 0$) has a contrary impact on $f'(\xi, \eta)$, $\theta(\xi, \eta)$, and $\phi(\xi, \eta)$ profiles, i.e., $\phi(\xi, \eta)$ profile decreases with Δ and, resultantly, $f'(\xi, \eta)$ profile also decreases in Fig. 15, but $\theta(\xi, \eta)$ pro-

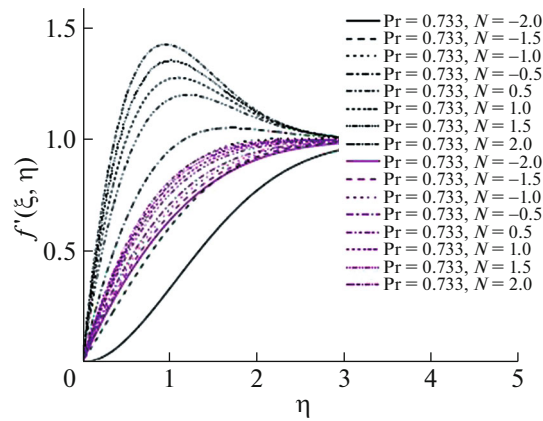


Fig. 18. $f'(\xi, \eta)$ profile for Pr and N .

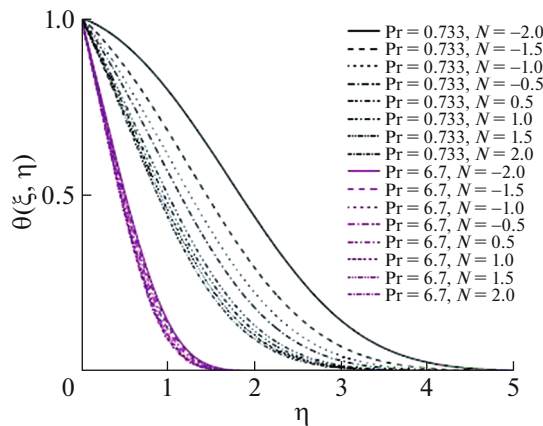


Fig. 19. $\theta(\xi, \eta)$ profile for Pr and N .

file has a little increment, see Fig. 16. In Figs. 15–17, $f'(\xi, \eta)$ and $\phi(\xi, \eta)$ profiles reduces with Sc , but $\theta(\xi, \eta)$ profile gained a little enhancement with Sc ; Sc is the ratio between kinematic viscosity and solute diffusivity and an increment in this means an increment in kinematic viscosity and reduction in solute diffusivity; Δ is the ratio between chemical reaction rate and kinematic viscosity, and an increment in this refers to an increment in chemical reaction rate and a reduction in kinematic viscosity; in Figs. 15–17, we can observe that impact of Δ reduced at $Sc = 2.57$ compared to $Sc = 0.66$ because of high kinematic viscosity; therefore, it can conclude that Δ is more realistic in low viscosity fluid.

Figures 18–20 proposes $f'(\xi, \eta)$, $\theta(\xi, \eta)$, and $\phi(\xi, \eta)$ profiles for Pr and N variation together with $Q = 1.0$, $\lambda = 1.0$, $m = 1/2$, $Sc = 0.66$, and $\Delta = 0.5$. In Fig. 18, $f'(\xi, \eta)$ profile increases with N (in the adding flow $N > 0$) and decreases in the opposing flow ($N < 0$), while in Figs. 19 and 20, $\theta(\xi, \eta)$ and $\phi(\xi, \eta)$ profiles decreases with N in the adding flow $N > 0$ and contrary in the opposing flow $N < 0$, i.e., increases. In Figs. 18–20, we observe that $f'(\xi, \eta)$, $\theta(\xi, \eta)$, and $\phi(\xi, \eta)$ profiles thickness is higher at $Pr = 0.733$ compared to $Pr = 6.7$; hence, we can conclude that the buoyancy ratio has dominating active-ness on flow quantities in low viscosity fluid.

Table 1 provides the governing parameters Pr, Sc , m , Δ , λ , N , and Q impacts on the C_f , Nu_x , and Sh_x with $Q = 1.0$, $Pr = 0.733$, $\lambda = 1.0$, $m = 1/2$, $N = 1.0$, $Sc = 0.66$, and $\Delta = 1.0$. An increment in Pr improves Nu_x and reduces C_f and Sh_x . C_f , Nu_x , and Sh_x flow quantities raise with an increment in m ; that means while we are increasing the cone half-angle that pushes the cone radius also and the surface of the cone acts as a blocker in the flow which causes the increment in skin friction, but it has a positive impact on Nu_x and Sh_x ; i.e., Nu_x and Sh_x rates enhanced because of the surface contact time increment.

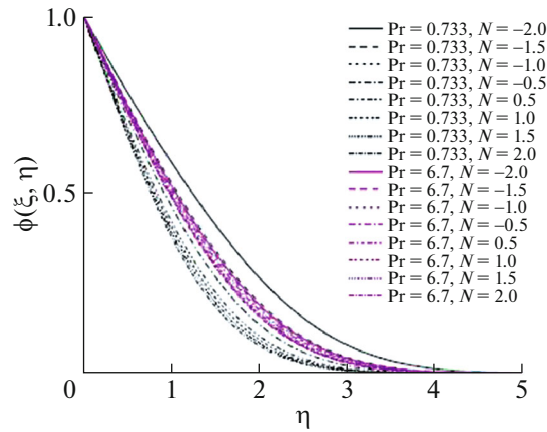


Fig. 20. $\phi(\xi, \eta)$ profile for Pr and N .

An impact of Δ (for consumption chemical reaction $\Delta < 0$) boosts C_f and Nu_x due to the slows down in fluid-particle acceleration we can predict it from Fig. 9; therefore, it impacts Sh_x in a little decrement, but in generation chemical reaction case $\Delta > 0$ these have reverse trend, i.e., C_f and Nu_x decrease, and Sh_x

Table 1. Influence of Pr, Sc, m , Δ , λ , N , and Q on C_f , Nu_x , and Sh_x with respect to Pr = 0.733, $\lambda = 1.0$, $m = 0.5$, Sc = 0.66, $Q = 1.0$, $N = 1.0$, and $\Delta = 0.5$, respectively

Pr	Sc	m	Δ	λ	N	Q	C_f	Nu_x	Sh_x
0.733	0.66	0.5	1.0	0.5	1.0	1.0	2.23545	0.17183	0.24662
6.7	0.66						0.92791	0.40342	0.20577
	2.57						2.23545	0.17183	0.24662
		0.2					2.03868	0.14962	0.20552
		0.3					2.09889	0.15682	0.21904
		0.5					2.23545	0.17183	0.24662
			-1.0				2.27532	0.17450	0.18482
			-0.5				2.26099	0.17354	0.20654
			0.5				2.23545	0.17183	0.24662
			1.0				2.22401	0.17107	0.26523
				1.0			2.23545	0.17183	0.24662
				3.0			4.42860	0.23437	0.29136
				5.0			6.28531	0.27163	0.31990
				7.0			7.96855	0.29916	0.34168
					-1.0		0.88035	0.10922	0.20693
					-0.5		1.25385	0.13006	0.21948
					0.5		1.92533	0.16012	0.23876
					1.0		2.23545	0.17183	0.24662
						-4.0	2.08831	0.42203	0.24025
						-3.0	2.10886	0.38184	0.24111
						-2.0	2.13262	0.33800	0.24212
						-1.0	2.16054	0.28951	0.24332
						1.0	2.23545	0.17183	0.24662
						2.0	2.28810	0.09667	0.24896
						3.0	2.35764	0.00321	0.25205
						4.0	2.45302	-0.11902	0.25625

increases. C_f , Nu_x , and Sh_x flow quantities enhance with λ and $N > 0$ but decreases with $N < 0$. Impact of Q ($Q < 0$ for heat absorption) enhances Nu_x but C_f and Sh_x reduces; for $Q < 0$ heat absorption is acted as a sink inflow region; therefore, the heat transfer from the surface of the cone to the flow region enhances; for $Q > 0$ (heat generation) Nu_x decreases, and for higher values of Q it took negative trend also which indicates when heat generation rate is higher than the heat is transferring from flow region to the surface, but C_f and Sh_x enhances.

5. CONCLUSIONS

Mixed convection flow of an incompressible viscous fluid across a vertical cone saturated porous medium with the heat source/sink and chemical reaction effects measured in this segment of contribution and reached to conclude follows:

- Impact of Q boosts Nu_x and slows down C_f and Sh_x for heat absorption ($Q < 0$); likewise, for heat generation ($Q > 0$) it boosts C_f and Sh_x and slows down Nu_x and turned heat transfer as flow to surface. $f'(\xi, \eta)$ and $\theta(\xi, \eta)$ profiles decrease with Q but $\phi(\xi, \eta)$ profile increases for $Q < 0$; likewise, $f'(\xi, \eta)$ and $\theta(\xi, \eta)$ profiles increase with Q but $\phi(\xi, \eta)$ profile decreases for $Q > 0$.
- An impact of $\Delta < 0$ (for chemical reaction consumption) boosts C_f and Nu_x , and decreases Sh_x but the impact of $\Delta > 0$ (for chemical reaction generation) decrease C_f and Nu_x , and increases Sh_x . $f'(\xi, \eta)$ and $\phi(\xi, \eta)$ profiles enhance with $\Delta < 0$ but $\theta(\xi, \eta)$ profile decreases; similarly, $\Delta > 0$ turns $f'(\xi, \eta)$, $\theta(\xi, \eta)$ and $\phi(\xi, \eta)$ profiles in a contrary way.
- All the C_f , Nu_x , and Sh_x quantities enhance with λ and N ($N > 0$ in adding flow case) but reduces in the opposing flow case ($N < 0$). $f'(\xi, \eta)$ profile enhances with both the λ and N , but $\theta(\xi, \eta)$ and $\phi(\xi, \eta)$ profiles decrease. Both the λ and N become more dominant in low viscosity fluid ($Pr = 0.733$) comparing to higher one ($Pr = 6.7$).
- C_f , Nu_x , and Sh_x flow quantities raise with an increment in m . $f'(\xi, \eta)$ profile decreases with m but $\theta(\xi, \eta)$ and $\phi(\xi, \eta)$ profiles enhance in low viscosity fluid ($Pr = 0.733$) but turned in reverse trend in higher viscosity fluid ($Pr = 6.7$).

CONFLICT OF INTEREST

The authors declare that they have no conflicts of interest.

REFERENCES

1. K. A. Yih, "Heat source/sink effect on MHD mixed convection in stagnation flow on a vertical permeable plate in porous media," *Int. Commun. Heat Mass Transfer* **25** (3), 427–442 (1998).
[https://doi.org/10.1016/S0735-1933\(98\)00030-X](https://doi.org/10.1016/S0735-1933(98)00030-X)
2. A. A. Mohammadein and R. S. R. Gorla, "Heat transfer in a micropolar fluid over a stretching sheet with viscous dissipation and internal heat generation," *Int. J. Numer. Methods Heat Fluid Flow* **11** (1), 50–58 (2001).
<https://doi.org/10.1108/09615530110364088>
3. F. S. Ibrahim, A. M. Elaiw, and A. A. Bakr, "Effect of the chemical reaction and radiation absorption on the unsteady MHD free convection flow past a semi infinite vertical permeable moving plate with heat source and suction," *Commun. Nonlinear Sci. Numer. Simul.* **13** (6), 1056–1066 (2008).
<https://doi.org/10.1016/j.cnsns.2006.09.007>
4. A. M. Salem and M. A. El-Aziz, "Effect of Hall currents and chemical reaction on hydromagnetic flow of a stretching vertical surface with internal heat generation/absorption," *Appl. Math. Modell.* **32** (7), 1236–1254 (2008).
<https://doi.org/10.1016/j.apm.2007.03.008>
5. S. S. Das, A. Satapathy, J. K. Das, and J. P. Panda, "Mass transfer effect on MHD flow and heat transfer past a vertical porous plate through a porous medium under oscillatory suction and heat source," *Int. J. Heat Mass Transfer* **52** (25–26), 5962–5969 (2009).
<https://doi.org/10.1016/j.ijheatmasstransfer.2009.04.038>
6. P. M. Patil, S. Roy, and A. J. Chamkha, "Double diffusive mixed convection flow over a moving vertical plate in the presence of internal heat generation and a chemical reaction," *Turk. J. Eng. Environ. Sci.* **33** (3), 193–205

- (2009).
<https://doi.org/10.3906/muh-0905-21>
7. P. M. Patil, S. Roy, and I. Pop, "Flow and heat transfer over a moving vertical plate in a parallel free stream: role of internal heat generation or absorption." *Chem. Eng. Commun.* **199** (5), 658–672 (2012).
<https://doi.org/10.1080/00986445.2011.614978>
 8. W. Ibrahim and B. Shanker, "Unsteady MHD boundary-layer flow and heat transfer due to stretching sheet in the presence of heat source or sink," *Comput. Fluids* **70**, 21–28 (2012).
<https://doi.org/10.1016/j.compfluid.2012.08.019>
 9. S. R. Mishra, G. C. Dash, and M. Acharya, "Mass and heat transfer effect on MHD flow of a visco-elastic fluid through porous medium with oscillatory suction and heat source," *Int. J. Heat Mass Transfer* **57** (2), 433–438 (2013).
<https://doi.org/10.1016/j.ijheatmasstransfer.2012.10.053>
 10. S. Jena, G. C. Dash, and S. R. Mishra, "Chemical reaction effect on MHD viscoelastic fluid flow over a vertical stretching sheet with heat source/sink," *Ain Shams Eng. J.* **9** (4), 1205–1213 (2018).
<https://doi.org/10.1016/j.asej.2016.06.014>
 11. S. H. Islam and N. Ahmed, "Effect of thermal diffusion and chemical reaction on MHD free convective flow past an infinite isothermal vertical plate with heat source," *Ital. J. Pure Appl. Math.* **42**, 559–574 (2019).
 12. B. Nayak, S. R. Mishra, and G. Gopi Krishna, "Chemical reaction effect of an axisymmetric flow over radially stretched sheet," *Propul. Power Res.* **8** (1), 79–84 (2019).
<https://doi.org/10.1016/j.jprr.2019.01.002>
 13. Muhaimin, R. Kandasamy and I. Hashim, "Effect of chemical reaction, heat and mass transfer on nonlinear boundary layer past a porous shrinking sheet in the presence of suction," *Nucl. Eng. Des.* **240** (5), 933–939 (2010).
<https://doi.org/10.1016/j.nucengdes.2009.12.024>
 14. M. K. Nayak, "Chemical reaction effect on MHD viscoelastic fluid over a stretching sheet through porous medium," *Meccanica* **51** (8), 1699–1711 (2016).
<https://doi.org/10.1007/s11012-015-0329-3>
 15. J. A. Rao and S. Shivaiah, "Chemical reaction effects on unsteady MHD flow past semi-infinite vertical porous plate with viscous dissipation," *Appl. Math. Mech. – Engl. Ed.* **32** (8), 1065–1078 (2011).
<https://doi.org/10.1007/s10483-011-1481-6>
 16. N. Mahapatra, G. C. Dash, S. Panda, and M. Acharya, "Effects of chemical reaction on free convection flow through a porous medium bounded by a vertical surface," *J. Eng. Phys. Thermophys.* **83** (1), 130–140 (2010).
<https://doi.org/10.1007/s10891-010-0327-1>
 17. N. Senapati, R. K. Dhal, and T. K. Das, "Effects of chemical reaction on free convection MHD flow through porous medium bounded by vertical surface with slip flow region," *Am. J. Comput. Appl. Math.* **2** (3), 124–135 (2012).
<https://doi.org/10.5923/j.ajcam.20120203.10>
 18. K. Bhattacharyya and G. C. Layek, "Similarity solution of MHD boundary layer flow with diffusion and chemical reaction over a porous flat plate with suction/blowing," *Meccanica* **47** (4), 1043–1048 (2012).
<https://doi.org/10.1007/s11012-011-9461-x>
 19. M. S. Abel, P. S. Datti, and N. Mahesha, "Flow and heat transfer in a power-law fluid over a stretching sheet with variable thermal conductivity and non-uniform heat source," *Int. J. Heat and Mass Transfer* **52** (11–12), 2902–2913 (2009).
<https://doi.org/10.1016/j.ijheatmasstransfer.2008.08.042>
 20. M. S. Abel, M. M. Nandeppanavar, and S. B. Malipatil, "Heat transfer in a second grade fluid through a porous medium from a permeable stretching sheet with non-uniform heat source/sink," *Int. J. Heat Mass Transfer* **53** (9–10), 1788–1795 (2010).
<https://doi.org/10.1016/j.ijheatmasstransfer.2010.01.011>
 21. D. Pal and S. Chatterjee, "Heat and mass transfer in MHD non-Darcian flow of a micropolar fluid over a stretching sheet embedded in a porous media with non-uniform heat source and thermal radiation," *Commun. Nonlinear Sci. Numer. Simul.* **15** (7), 1843–1857 (2010).
<https://doi.org/10.1016/j.cnsns.2009.07.024>
 22. M. M. Nandeppanavar, K. Vajravelu, M. S. Abel, and C.-O. Ng, "Heat transfer over a nonlinearly stretching sheet with non-uniform heat source and variable wall temperature," *Int. J. Heat Mass Transfer* **54** (23–24), 4960–4965 (2011).
<https://doi.org/10.1016/j.ijheatmasstransfer.2011.07.009>
 23. N. F. M. Noor, S. Abbasbandy, and I. Hashim, "Heat and mass transfer of thermophoretic MHD flow over an inclined radiate isothermal permeable surface in the presence of heat source/sink," *Int. J. Heat Mass Transfer* **55** (7–8), 2122–2128 (2012).
<https://doi.org/10.1016/j.ijheatmasstransfer.2011.12.015>

24. R. Sharma, "Effect of viscous dissipation and heat source on unsteady boundary layer flow and heat transfer past a stretching surface embedded in a porous medium using element free Galerkin method," *Appl. Math. Comput.* **219** (3), 976–987 (2012).
<https://doi.org/10.1016/j.amc.2012.07.002>
25. D. Srinivasacharya, J. Pranitha, and Ch. RamReddy, "Magnetic effect on free convection in a non-Darcy porous medium saturated with doubly stratified power-law fluid," *J. Braz. Soc. Mech. Sci. Eng.* **33** (1), 8–14 (2011).
<https://doi.org/10.1590/S1678-58782011000100002>
26. F. Mabood, S. M. Ibrahim, M. M. Rashidi, M. S. Shadloo, and G. Lorenzini, "Non-uniform heat source/sink and Soret effects on MHD non-Darcian convective flow past a stretching sheet in a micropolar fluid with radiation," *Int. J. Heat Mass Transfer* **93**, 674–682 (2016).
<https://doi.org/10.1016/j.ijheatmasstransfer.2015.10.014>
27. T. Hayat, S. Qayyum, A. Alsaedi, and A. Shafiq, "Inclined magnetic field and heat source/sink aspect in flow of nanofluid with nonlinear thermal radiation," *Int. J. Heat Mass Transfer* **103**, 99–107 (2016).
<https://doi.org/10.1016/j.ijheatmasstransfer.2016.06.055>
28. O. P. Meena, "Mixed convection nanofluid flow over a vertical wedge saturated in porous media with the influence of thermal dispersion using Lie group scaling," *Comput. Therm. Sci.: Int. J.* **12** (3), 91–105 (2020).
<https://doi.org/10.1615/ComputThermalScien.2020032330>
29. O. P. Meena, "Mixed convection nanofluid flow over a vertical wedge saturated in porous medium with influence of double dispersion using Lie group scaling," *Spec. Top. Rev. Porous Media—Int. J.* **11** (3), 297–311 (2020).
<https://doi.org/10.1615/SpecialTopicsRevPorousMedia.2020031755>
30. O. P. Meena and J. Pranitha, "Power-law nanofluid on mixed convection with influence of double dispersion saturated non-Darcy porous media," *AIP Conf. Proc.* **2246**, 020019 (2020).
<https://doi.org/10.1063/5.0014503>
31. J. Pranitha and O. P. Meena, "Influence of double dispersion on natural convection flow over a vertical cone saturated porous media with Soret and Dufour effects," *Int. J. Eng. Sci. (IJES)* **2**, 9–15, 2020.
32. O. P. Meena, P. Janapatla, and A. J. Chamkha, "Influence of the Soret and Dufour on mixed convection flow over a vertical cone with injection/suction effects," *J. Porous Media* **24** (4), 73–88 (2021).
<https://doi.org/10.1615/JPorMedia.2021034700>
33. O. P. Meena, "Mixed convection flow over a vertical cone with double dispersion and chemical reaction effects," *Heat Transfer Res.* **50** (5), 4516–4534 (2021).
<https://doi.org/10.1002/htj.22086>
34. O. P. Meena, P. Janapatla, and M. K. Meena, "Influence of thermal dispersion and chemical reaction on mixed convection flow over a vertical cone saturated porous media with injection/suction," *Math. Models Comput. Simul.* **14** (1), 172–185 (2022).
<https://doi.org/10.1134/S2070048221060144>
35. O. P. Meena, "Influence of injection/suction on mixed convection flow across a vertical cone saturated porous medium with double dispersion and chemical reaction effects," *Tec. Ital.* **65** (2–4), 433–441, 2021.
<https://doi.org/10.18280/ti-ijes.652-442>
36. O. P. Meena, P. Janapatla, and D. Srinivasacharya, "Influence of Soret and Dufour on mixed convection flow across a vertical cone," *Heat Transfer Res.* **50** (8), 8280–8300 (2021).
<https://doi.org/10.1002/htj.22277>
37. R. Ravindran, S. Roy, and E. Momoniat, "Effects of injection (suction) on a steady mixed convection boundary layer flow over a vertical cone," *Int. J. Numer. Methods Heat Fluid Flow* **19** (3/4), 432–444 (2009).
<https://doi.org/10.1108/09615530910938362>
38. K. A. Yih, "Mixed convection about a cone in a porous medium: the entire region," *Int. Commun. Heat Mass Transfer* **26** (7), 1041–1050 (1999).
39. O. P. Meena, "Spectral quasilinearization method for a porous channel problem with micropolar flow," *J. Compos. Theory* **12** (9), 40–45 (2019).
40. O. P. Meena, J. Pranitha, and D. Srinivasacharya, "Mixed convection fluid flow over a vertical cone saturated porous media with double dispersion and injection/suction effects," *Int. J. Appl. Comput. Math.* **7** (3), 59 (2021).
<https://doi.org/10.1007/s40819-021-00990-y>
41. V. M. Magagula, S. S. Motsa, and P. Sibanda, "A new bivariate spectral collocation method with quadratic convergence for systems of nonlinear coupled differential equations," *Appl. Comput. Math.* **18** (2), 113–122 (2019).
42. R. Ravindran and M. Ganapathirao, "Non-uniform slot suction/injection into mixed convection boundary layer flow over vertical cone," *Appl. Math. Mech. — Engl. Ed.* **34** (11), 1327–1338 (2013).
<https://doi.org/10.1007/s10483-013-1748-7>